Turnover of microbial lipids in the deep biosphere and growth of benthic archaeal populations

Sitan Xie[a], Julius S. Lipp[a], Gunter Wegener[b,c], Timothy G. Ferdelman[c], and Kai-Uwe Hinrichs[a,1]

[a]Organic Geochemistry Group, MARUM-Center for Marine Environmental Sciences and Department of Geosciences, University of Bremen, D-28359 Bremen, Germany; [b]Alfred Wegener Institute for Polar and Marine Research, Research Group for Deep Sea Ecology and Technology, D-27515 Bremerhaven, Germany; and [c]Max Planck Institute for Marine Microbiology, D-28359 Bremen, Germany

Edited by Edward F. DeLong, Massachusetts Institute of Technology, Cambridge, MA, and approved February 21, 2013 (received for review October 24, 2012)

Deep subseafloor sediments host a microbial biosphere with unknown impact on global biogeochemical cycles. This study tests previous evidence based on microbial intact polar lipids (IPLs) as proxies of live biomass, suggesting that Archaea dominate the marine sedimentary biosphere. We devised a sensitive radiotracer assay to measure the decay rate of ([^{14}C]glucosyl)-diphytanylglyceroldiether (GlcDGD) as an analog of archaeal IPLs in continental margin sediments. The degradation kinetics were incorporated in model simulations that constrained the fossil fraction of subseafloor IPLs and rates of archaeal turnover. Simulating the top 1 km in a generic continental margin sediment column, we estimated degradation rate constants of GlcDGD being one to two orders of magnitude lower than those of bacterial IPLs, with half-lives of GlcDGD increasing with depth to 310 ky. Given estimated microbial community turnover times of 1.6–73 ky in sediments deeper than 1 m, 50–96% of archaeal IPLs represent fossil signals. Consequently, previous lipid-based estimates of global subseafloor biomass probably are too high, and the widely observed dominance of archaeal IPLs does not rule out a deep biosphere dominated by Bacteria. Reverse modeling of existing concentration profiles suggest that archaeal IPL synthesis rates decline from around 1,000 pg·mL^{-1} sediment·y^{-1} at the surface to 0.2 pg·mL^{-1}·y^{-1} at 1 km depth, equivalent to production of 7×10^5 to 140 archaeal cells·mL^{-1} sediment·y^{-1}, respectively. These constraints on microbial growth are an important step toward understanding the relationship between the deep biosphere and the carbon cycle.

diagenetic model | marine sediment | phospholipid-derived fatty acid

Deep marine sediments host a large microbial population (1). Estimates of cellular carbon in subseafloor sediments range from 4 to 303 Pg C (2–5). Recalcitrant organic matter is considered to constitute the major source of metabolic energy (1). Estimates of turnover times of microbial populations in the subseafloor range from hundreds to thousands of years (3, 6, 7).

Intact polar lipids (IPLs) of both Archaea and Bacteria have been proposed as life markers of microbes in sediments and soils (8, 9). Because of the reactivity of the bond linking the polar head group to the glycerol backbone of IPLs, these are assumed to be unstable after cellular decay (10–12) and therefore have been applied as proxies for live microbial cells in a variety of ecosystems (e.g., refs. 4, 9, 13, and 14). The value of an IPL as a life marker depends on the fate of extracellular IPLs, i.e., compounds no longer associated with intact cells that may accumulate as molecular fossils, and more specifically, on the relationship between the turnover time of extracellular IPLs and that of cellular biomass.

In marine subseafloor sediments, archaeal IPLs generally are more abundant than their bacterial counterparts (4, 6, 15). This observation led to the suggestion that Archaea are the dominant microbial domain in this habitat (4, 6). The predominant archaeal IPL type consists of glycosidic ether lipids, whereas phosphate ester–based IPLs commonly found in Bacteria and Eukarya, so-called phospholipids, rarely are detected in deeply buried subseafloor sediments (4, 6, 15). This dominance of one structurally distinct IPL type raised questions regarding the suitability of glycosidic IPLs as proxies for live biomass in the deep biosphere (15, 16).

Previous experiments on IPL degradation showed generally higher degradation rate constants for bacterial/eukaryal phospholipids vs. archaeal IPLs (11, 12, 17). Although these experiments generally are informative in qualitative terms, their relevance to exploring the fate of microbial IPLs in the deep biosphere is limited because studies either were conducted as relatively short incubations of active surface sediments, partially under aerobic conditions (11), or monitored the declining concentration of IPLs, which resulted in noisy data with high uncertainties, especially for the more slowly decaying archaeal IPLs (12, 17); this circumstance prevented extrapolation to longer time scales. In addition, the recent 100-d–long degradation experiment of archaeal IPLs did not encompass the glycolipids typically found in subseafloor sediments (12).

Laboratory-based simulation of biogeochemical processes operating on geological time scales, such as IPL turnover in the deep biosphere, is inherently difficult, and residual uncertainties are a consequence. High-quality experimental data on the degradation kinetics of relevant IPLs under suitable conditions are required to establish models that simulate the turnover of IPLs and, by inference, microbial turnover. Two recent studies quantitatively examined turnover of archaeal IPLs but without using informed estimates of the degradation kinetics under sedimentary conditions. For example, Lipp and Hinrichs (15) assumed IPL half-lives (1–500 ky in a hypothetical 1-km sediment column) to be in the general range of existing estimates of subseafloor community turnover times. Schouten et al. (16) examined a scenario in which degradation of water column–derived archaeal glycolipids without sedimentary in situ production governs the IPL concentration profile and argued against the necessity of in situ production because of the striking similarity of the IPL regression line (4) and an empirical total organic carbon (TOC) decay function (18)—a phenomenon to be expected if glycosidic archaeal IPLs were to degrade with kinetics similar to those of bulk TOC; the corresponding IPL half-lives in a hypothetical 1-km sediment column ranged from 2 ky to 220 My [a = 0.22, b = 1 (16); Eqs. **S4A** and **S11A** when b = 1].

Given the above-mentioned uncertainties regarding the fate of microbial lipids in the subseafloor, we designed a highly sensitive radiotracer assay for determining the degradation rate during 300-d incubation of the partially ^{14}C-labeled compound ([^{14}C]glucosyl)-diphytanylglyceroldiether (GlcDGD); Fig. 1*A*] using a shallow-water surface sediment and a deeply buried continental margin sediment; we induced methanogenic conditions to

Author contributions: J.S.L., T.G.F., and K.-U.H. designed research; S.X., J.S.L., G.W., T.G.F., and K.-U.H. performed research; S.X., J.S.L., and K.-U.H. analyzed data; and S.X. and K.-U.H. wrote the paper.

The authors declare no conflict of interest.

This article is a PNAS Direct Submission.

[1]To whom correspondence should be addressed. E-mail: khinrichs@uni-bremen.de.

This article contains supporting information online at www.pnas.org/lookup/suppl/doi:10.1073/pnas.1218569110/-/DCSupplemental.

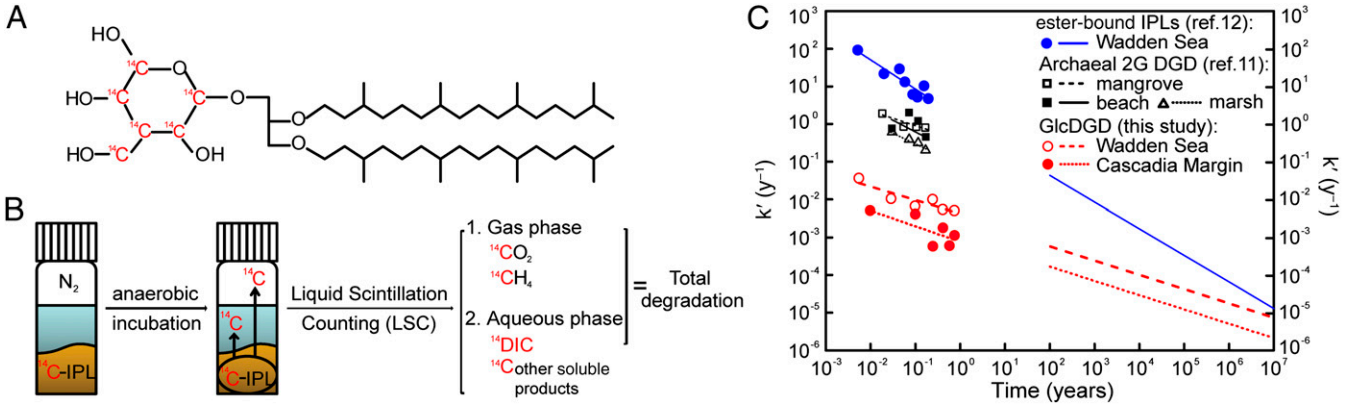

Fig. 1. Determination of the degradation kinetics of GlcDGD and resulting degradation constants as a function of time. (*A*) Molecular structure of partially radiolabeled GlcDGD that serves as a model compound for prominent sedimentary archaeal IPLs. (*B*) Flow sketch of the anaerobic incubation experiment. (*C*) Relationship of degradation constant (k′) of GlcDGD (this study), ester-bound IPLs (12) (representative of typical bacterial IPLs), and archaeal diglycosyl (2G) DGD (11) (anaerobic incubation in mangrove, beach, and marsh sediment). ○ and ●, k′ values determined from experimental results. Lines for t < 1 y were derived via linear fitting between calculated k′ and t (Eq. **S2**); lines for t > 100 y represent modeling results based on reverse fitting of experimental results (Eq. **S4**; see *II. SI Text*, section II.1 for details). The gap is a result of the minimum age of the modeled sediment column (Fig. 2) of 100 y.

mimic low–metabolic energy conditions presumed to prevail in large volumes of continental margin sediments that are situated below the sulfate–methane transition zone (19). GlcDGD served as model compound for the most abundant class of archaeal IPLs. In a next step, we assessed the validity of IPLs as proxies of subseafloor biomass by simulating concentration profiles of archaeal and bacterial lipids in a generic continental margin subseafloor sediment column. In this model, the production rate of microbial lipids was linked to the decay rate of TOC and degradation rates of IPLs were computed on the basis of experimentally derived degradation rate constants. In an independent model, we estimated the sedimentary production rates of archaeal lipids required to balance the experimentally determined decay rates to account for observed subseafloor lipid profiles (4). Collectively, this study provides unique quantitative information regarding the significance of microbial lipid distributions in subseafloor sediments and constrains the turnover of subseafloor microbial populations.

Results and Discussion

Degradation Kinetics of IPLs in the Deep Biosphere. Partially ^{14}C-labeled GlcDGD enabled us to monitor hydrolysis of its glycosidic bond during anaerobic incubation in both surface and subseafloor sediment from the German Wadden Sea and the Cascadia Margin, respectively. The premise of the experiment is that intact GlcDGD is largely insoluble in water, whereas ^{14}C-labeled products resulting from cleavage of the polar headgroup are either highly water soluble (^{14}C-dissolved inorganic carbon [DIC], [^{14}C]glucose, and degradation products of glucose) or detectable in the gas phase ([^{14}C]CO_2, [^{14}C]CH_4) (compare Fig. 1). However, because of the slight solubility (equivalent to 2% of initial radioactivity) of GlcDGD in water and the lack of significant radioactivity change during the experiment, the potential release and accumulation of radioactive organic intermediates were not detectable (Fig. S1). This is consistent with observations by Harvey et al. (11), who barely detected intermediates during degradation of archaeal IPLs. Consequently, degraded products were detected only as radioactive DIC, CH_4, and CO_2. The reported degradation rates thus are minimum estimates; actual rates may be slightly higher. After 300-d incubation, 0.5% GlcDGD was degraded in Wadden Sea sediment, whereas only 0.15% was degraded in Cascadia Margin subsurface sediment (Fig. S1).

A large majority of the diagenetic reactions and processes in marine sediments are related either directly or indirectly to the degradation of TOC (18), which follows first-order kinetics (18). The degradation rate of IPLs (IPL_{deg}) in sediments also may be described by first-order kinetics (Eq. **S1**; see *II. SI Text*, section II.1, where all calculations are reviewed), using a degradation rate constant k′ that decreases with time (12, 16) (Eqs. **S2–S4** and Table S1). For experimental observations, values of k′ of ester-bound IPLs are two to four orders of magnitude higher than those of GlcDGD, whereas k′ of GlcDGD is an order of magnitude higher in surface sediment than in subsurface sediment (Fig. 1*C*).

Simulation of the fate of IPLs in the deep biosphere requires extrapolation of k′ to a geological time scale (Fig. 1*C*; *II. SI Text*, sections II.1 and II.2; and Figs. S2–S4). Extrapolated values of k′ for both ester-bound IPLs and GlcDGD decline with depth but converge as the result of different slopes b′; k′ values of GlcDGD in both surface and subsurface sediment remain lower than those of ester-bound IPLs for at least 10^7 years (Fig. 1*C*). The effect of presumed higher microbial activity in the Wadden Sea surface sediment is reflected in around four to five times higher k′ values of GlcDGD relative to Cascadia Margin sediment in the projected time interval. Even higher values of k′ were obtained previously in shorter degradation experiments of diglycosyl-DGD using mangrove, beach, and marsh sediment (11; Fig. 1*C*).

Potential uncertainties induced by the extrapolation to geologic time scales require careful examination of propagated errors caused by reverse fitting of experimental results for the determination of a′ and b′. The methodology and consequences for subsequent models are discussed in *II. SI Text*, section II.2 and illustrated in Figs. S2–S4. The uncertainties are generally larger for extrapolations of k′ for GlcDGD compared with ester-bound IPLs, with the consequence that we can confidently predict k′ within less than two orders of magnitude for 10-My-old sediments (Figs. S3 and S4).

Simulation of IPL Profiles in the Deep Biosphere and Implications for Subseafloor Life. Simulation of the effect of different values of k′ on vertical sediment profiles of archaeal and bacterial IPLs requires reasonable estimates of their production rates in the subseafloor. We simulated the production of IPLs in a generic model sequence of continental margin sediment under the assumption that microbial growth and lipid biosynthesis are tightly linked to the degradation kinetics of TOC. For this purpose, we

used a diagenetic model of TOC decay (20) that has been validated independently as widely applicable (21). Detailed parameters used in the model are presented in *II. SI Text*, sections II.3–II.5. In brief, sedimentation rates are set to 10 cm·ky^{-1}, TOC concentration at the sediment surface is set to 1%, and decreases in response to simulated degradation are set to 0.2% at 1 km subseafloor depth (Fig. 2*A* and *II. SI Text*, section II.3). The biomass of microbial populations is scaled with the free-energy yield of the used metabolic reaction (22), which is considered to be minimal in the deep biosphere (19). We converted the rate of degraded TOC into microbial biomass using carbon assimilation efficiencies of 1%; such low values have been established for anaerobic methanotrophic archaea (23, 24) that metabolize close to the biological energy quantum (25); 1/13 of the assimilated carbon is flowing into biosynthesis of IPLs (4, 26) (*II. SI Text*, section II.4). For the sake of illustrating the fate of both archaeal and bacterial IPLs, we divided the flow of carbon from microbial cells equally between Archaea and Bacteria; other ratios resulted in qualitatively similar results. Consequently, the resulting microbial biomass should comprise equal portions of both domains if the respective cellular populations turn over at equal rates.

The simulated rate of IPL production, $IPL_{pro\text{-}TOC}$, decreases with depth from 90 to 0.02 pg·mL^{-1} sediment·y^{-1} in the 1-km sediment column (Fig. 2*B*). IPL concentration then was modeled using a simple box-model that assumes that IPL concentration at each depth interval is represented by an input ($IPL_{pro\text{-}TOC}$) and an output (IPL_{deg}) flux (15) (Eq. **S10** and Fig. 2 *B* and *C*). The resulting profiles exhibit some of the general features also found in a compilation of widely distributed IPL profiles (Fig. 2*C*) (4). For example, the concentrations of archaeal IPLs exceed those of their bacterial counterparts by up to two orders of magnitude in sediments below 1 meters below seafloor (mbsf). The minimum of simulated bacterial IPL concentration in the top 5 cm was caused by a higher rate of degradation relative to production and results from the high starting concentration of IPLs at the sediment surface, which is defined by the regression (4) and regulates degradation (Eq. **S1**). The predicted concentration profiles of archaeal and bacterial IPLs fall in the general concentration ranges also observed in nature. These general trends remain largely unchanged when we consider the error propagation related to our extrapolation of k′ (Figs. S2–S4). This simulation thus demonstrates that typical sedimentary IPLs applied as proxy for microbial biomass and its taxonomic composition would overestimate both total biomass and the proportion of Archaea. We therefore suggest that currently the most realistic estimates of archaeal vs. bacterial biomass are derived from refined DNA-based techniques (4, 27, 28); accordingly, Bacteria are similarly abundant as Archaea, although predominance of one domain may occur in specific environments.

The comparison of our simulated microbial biomass production with the global regression of cellular counts (1) constrains the turnover of pools of IPLs and cells as well as the fossil fractions of the different IPL types (Fig. 3), keeping in mind the limitation that the samples included in the global data set of subseafloor cells (1) may not be ideally represented by the boundary conditions in our model. Biomass turnover times generally range from 1.6 to 73 ky. The steep decrease of cell concentrations in the top meter (1) combined with the relatively low decrease of $IPL_{pro\text{-}TOC}$ [derived from TOC degradation (20)] result in the minimum of biomass turnover at 1 mbsf. Because the turnover times of archaeal IPL pools exceed biomass turnover times for sediments below 0.1 mbsf (Fig. 3*A*), fossil, noncellular archaeal IPLs accumulate to the effect that only 4–50% represent intact cells below a depth of 1 mbsf (Fig. 3*B*). On the other hand, the rapid turnover of bacterial ester-bound IPLs relative to biomass turnover qualify them as useful markers for live bacterial cells in the deep biosphere. The size of fractions of cellular and noncellular archaeal IPLs is controlled by IPL turnover. Therefore, the shape of the curve of cellular IPLs (Fig. 3*B*) is related to the relationship between production rate and degradation rate (Fig. 2*B*). For example, maximum noncellular IPLs are expected in intervals in which production exceeds degradation; this is the case at around 5–10 mbsf in our simulation, in which the cellular component approaches a few percent. In both shallower and more deeply buried sediment, archaeal IPL production is lower than degradation (Fig. 2*B*), which results in higher proportions of cellular archaeal IPLs (Fig. 3*B*). Accordingly, in sediment deeper than 100 mbsf, the fossil fraction of archaeal IPLs is projected to be lower than 70–90%, depending on the kinetics used (Fig. 3*B*).

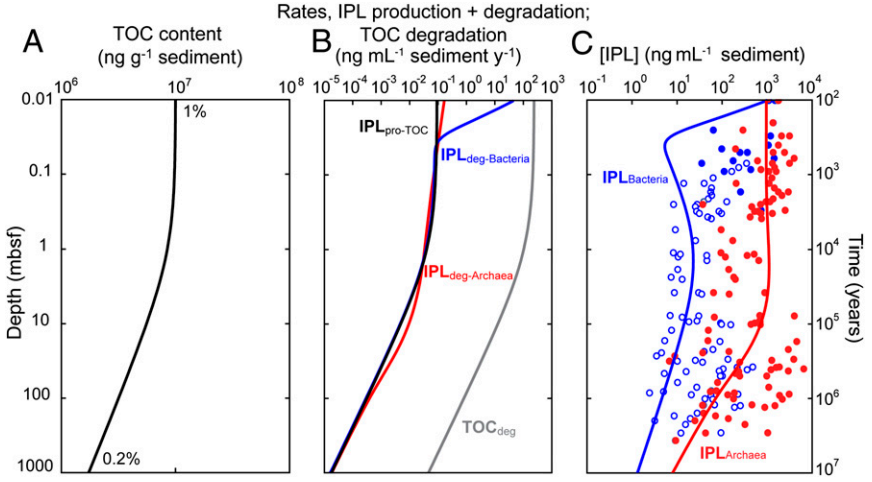

Fig. 2. Production, decay, and concentrations of IPLs in a model that simulates microbial growth linked to the degradation of TOC in a generic continental margin sediment column. (*A*) Depth (age) profile of TOC concentration derived from diagenetic modeling of TOC decay using first-order kinetics (20). (*B*) Depth profile of corresponding rates of TOC degradation, modeled production of bacterial and archaeal IPLs energetically linked to TOC decay, degradation rates of bacterial IPLs (based on extrapolation of experimental data from ref. 12), and degradation rates of archaeal IPLs using degradation kinetics of Cascadia Margin sediment (compare Fig. S4 for simulation with Wadden Sea kinetics). (*C*) Modeled concentration of archaeal and bacterial IPLs. Blue and red ●, observed concentrations of bacterial and archaeal IPLs (4); blue ○, maximum concentration of bacterial IPLs considering the analytical limit of detection (4). See text for model assumptions and methodology.

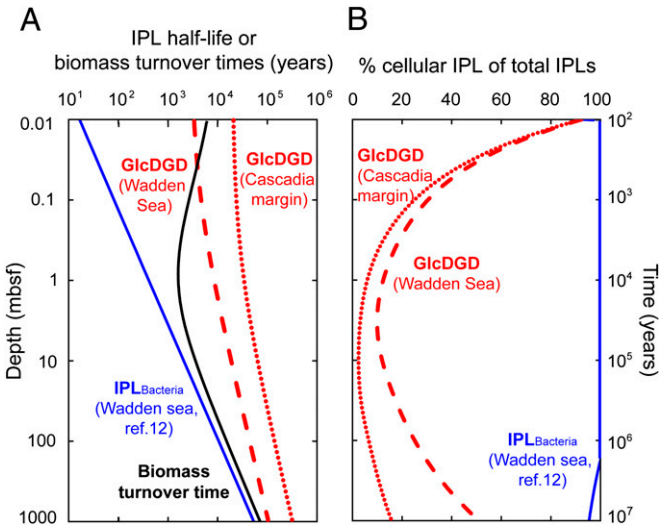

Fig. 3. Turnover times of biomass and IPLs and relative fractions of cellular IPLs for GlcDGD and bacterial IPLs. (*A*) Modeled half-life of archaeal and bacterial IPLs (Eq. **S11B**) based on degradation kinetics obtained from our degradation experiment and literature data [ester-bound IPLs (12)]. Biomass turnover time (black curve) is the time required to accumulate the cellular concentrations derived from the global regression line of direct cell counts (1) when converting $IPL_{pro\text{-}TOC}$ into cell concentration (Eq. **S12**). (*B*) Percentage of cellular IPLs in subseafloor sediment, derived from dividing cell concentrations from the global regression line for each depth interval (1) (converted to IPL concentration) through modeled IPL concentration (Fig. 2 and Eq. **S10**; see *II. SI Text*, section II.5 for details).

Constraints on Growth Rates of Archaeal Populations in Subseafloor Sediments. Independent of the above-described limitations of IPLs as proxies for the abundance of archaeal cells in deep subseafloor sediments, the degradation kinetics provide new constraints regarding the growth rates of archaeal populations. The experimentally determined kinetics of GlcDGD now enable us to extend a previous model (15) and demonstrate that in situ production of archaeal IPLs in subseafloor sediments is required to balance degradation; otherwise, the pool of archaeal IPLs would tend toward nondetectable levels at depths between 10 and 100 mbsf (Fig. 4*A*), and the general trends observed in subseafloor sediments (4) could not be reproduced. Although it is mathematically possible to generate a solution that does not require in situ production (16), the corresponding half-lives for the degradation of archaeal IPLs (2 ky to 220 My in the top 1 km) are inconsistent with our experimental data and probably unrealistic.

Estimates of the required production rates were derived by reverse fitting (*II. SI Text*, section II.6 and Eq. **S15**). The rates required to fit the concentration profile of archaeal IPLs closely to the IPL regression line (4) (Fig. 4*A*; see *II. SI Text*, section II.6 for details) decrease from 1 ng IPL·mL^{-1} sediment·y^{-1} at the sediment surface to ~0.2 pg IPL·mL^{-1} sediment·y^{-1} at 1,000 mbsf. Experimental evidence from a stable isotope-probing experiment with an 8-m–deep subseafloor sample from Cascadia Margin (29) provides independent support for the modeled growth rates (Fig. 4*B*). Conversion of IPLs to archaeal cells yields corresponding population growth rates, e.g., at 100 mbsf an annual growth of ~1,000 archaeal cells·mL^{-1} sediment is consistent with the IPL concentrations represented by the regression line. Although the uncertainties induced by the extrapolation of the degradation rate constant to geologic time scales need to be considered, the resulting biomass turnover times of microbial populations are broadly consistent with estimates based on other methods. For example, using the model based on TOC degradation (Fig. 2), we obtain a biomass turnover time of 15,500 y for sediments at 100 mbsf. If we assume that 50% of the cellular population consists of Archaea (cf. 4, 27, 28) and use the reverse model that matches lipid production to the cell-vs.-depth regression line (1), we obtain a range of 1,200–4,800 y of biomass turnover for the archaeal community. For comparison, Lomstein et al. (7) estimated a few hundred to 12,000 y for high-TOC sediments at the Peru Margin. When comparing our two model simulations, the higher biomass turnover times in the TOC-based model directly result from its lower lipid production rates compared with the reverse model (compare Figs. 2*B* and 4*B*). A plausible explanation for this difference is the bias of our IPL dataset (4) toward high-TOC sediment off the Peru Margin, which is associated with higher microbial activity, growth, and lipid production.

On the basis of newly determined experimental data on the degradation kinetics of a glycosidic glyceroldiether lipid resembling the properties of typical archaeal membrane lipids found ubiquitously in marine sediments, we conclude that a substantial portion of the archaeal IPLs found in subseafloor sediments are probably fossil products of past cell generations. Consequently, previous estimates of subseafloor biomass based largely on archaeal IPLs (4) were probably too high. Two independent model simulations of decay and production of microbial IPLs in the subseafloor established a quantitative framework that (*i*) demonstrates the effects of different degradation kinetics on concentration profiles of typical microbial lipids and (*ii*) provides constraints on the activity of the subseafloor biosphere. Our study highlights the challenges of distinguishing between bio- and geomolecules in

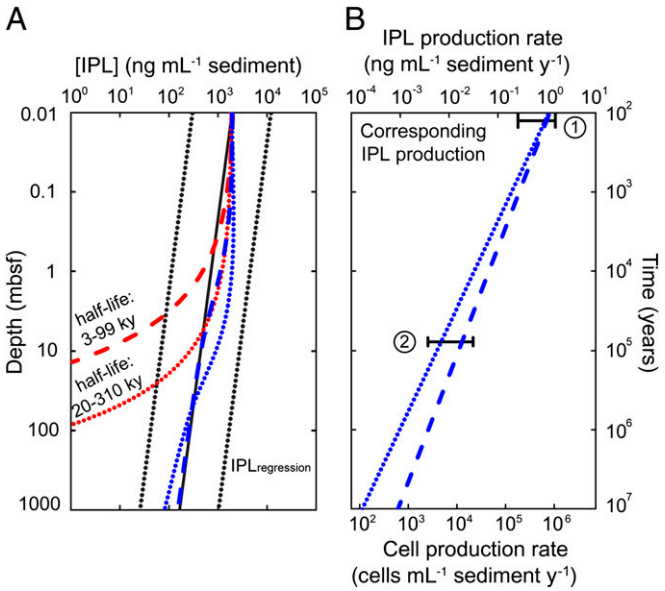

Fig. 4. Archaeal IPL production rates and corresponding population growth rates consistent with observed IPL concentration profiles. (*A*) Red curves, IPL concentration profile of a generic continental margin sediment column with input of IPLs limited to surface sediment (red dotted curve, degradation kinetics of GlcDGD in Cascadia Margin sediment; red dashed curve, degradation kinetics of GlcDGD in Wadden Sea sediment); blue curves, simulated IPL concentrations with production of archaeal IPLs balancing degradation for the two scenarios from red curves. Black solid line is regression and black dotted lines are 95% prediction intervals of observed IPL concentration (4). (*B*) Corresponding IPL production rates required to obtain the concentration profile of the blue curves in *A*. The IPL production rate at surface sediment is set to be 1 ng·mL^{-1} sediment·y^{-1}, which was determined in a recent stable isotope-probing study for coastal sediments younger than 100 y (31). The range of observations in that study is indicated by bar 1; bar 2 designates the range of IPL production rates (0.006–0.031 ng·g^{-1} sediment·y^{-1}) determined in a stable isotope-probing study using a subseafloor sample at 8 mbsf from Cascadia Margin (29). See text for model assumptions and methodology.

the deep sedimentary biosphere; these factors should be taken into consideration in the microbial ecological studies based on molecular techniques and may equally complicate assays based on other types of biomolecules, such as DNA (e.g., refs. 30 and 32) and cell wall components (7).

Materials and Methods

Samples are from the upper tidal flat of the Wadden Sea and the deep methanogenic subseafloor from Cascadia Margin [Integrated Ocean Drilling Program site U1326, 138.2 mbsf (33)]. Sediment slurries were prepared by mixing the sediment with an equal volume of sterilized, sulfate-free artificial seawater under anoxic conditions. Sterilized slurries were used as a control for nonbiological degradation of the IPLs. Four-milliliter slurry aliquots were incubated under N_2 headspace with 3.4 μCi (45 ng/mL sediment slurry) of [^{14}C] GlcDGD in the dark at in situ temperature (4 °C and 20 °C) for 300 d. The sterilized slurry was stored at 20 °C. At each time point, samples were taken in triplicate for radioactivity measurements of [^{14}C]CO_2, [^{14}C]CH_4, and ^{14}C-DIC to monitor degradation (further details are provided in *I. SI Materials and Methods*, section I.4; the models are described in the main text and *II. SI Text*).

ACKNOWLEDGMENTS. We thank the participating crews and scientists for sample recovery, Verena Heuer for sample donation, and Gabriele Schüßler, Marc Lamshöft, and Nguyen Manh Thang for technical support. Marshall Bowles and Matthias Zabel provided helpful comments on an earlier version of this paper. The sediment sample from the Cascadia Margin was provided by Integrated Ocean Drilling Program Expedition 311. This work was supported by the Deutsche Forschungsgemeinschaft through Projects Hi 616/11 and Li 1901/1 (S.X., J.S.L., and K.-U.H.) and through the Research Center/Cluster of Excellence MARUM-Center for Marine Environmental Sciences (all authors). Synthesis of the GlcDGD used funds from the European Research Council (ERC) under the European Union's Seventh Framework Programme—"Ideas" Specific Programme, ERC Grant 247153 (to K.-U.H.). S.X. was funded by the China Scholarship Council, and G.W. was funded by the Max Planck Society and the Gottfried Wilhelm Leibniz Prize (awarded to Antje Boetius).

1. Parkes RJ, Cragg BA, Wellsbury P (2000) Recent studies on bacterial populations and processes in subseafloor sediments: A review. *Hydrogeol J* 8(1):11–28.
2. Kallmeyer J, Pockalny R, Adhikari RR, Smith DC, D'Hondt S (2012) Global distribution of microbial abundance and biomass in subseafloor sediment. *Proc Natl Acad Sci USA* 109(40):16213–16216.
3. Whitman WB, Coleman DC, Wiebe WJ (1998) Prokaryotes: The unseen majority. *Proc Natl Acad Sci USA* 95(12):6578–6583.
4. Lipp JS, Morono Y, Inagaki F, Hinrichs K-U (2008) Significant contribution of Archaea to extant biomass in marine subsurface sediments. *Nature* 454(7207):991–994.
5. Parkes RJ, et al. (1994) Deep bacterial biosphere in Pacific Ocean sediments. *Nature* 371(6496):410–413.
6. Biddle JF, et al. (2006) Heterotrophic Archaea dominate sedimentary subsurface ecosystems off Peru. *Proc Natl Acad Sci USA* 103(10):3846–3851.
7. Lomstein BA, Langerhuus AT, D'Hondt S, Jørgensen BB, Spivack AJ (2012) Endospore abundance, microbial growth and necromass turnover in deep sub-seafloor sediment. *Nature* 484(7392):101–104.
8. Zink K-G, Wilkes H, Disko U, Elvert M, Horsfield B (2003) Intact phospholipids-microbial "life markers" in marine deep subsurface sediments. *Org Geochem* 34(6):755–769.
9. Sturt HF, Summons RE, Smith K, Elvert M, Hinrichs K-U (2004) Intact polar membrane lipids in prokaryotes and sediments deciphered by high-performance liquid chromatography/electrospray ionization multistage mass spectrometry—new biomarkers for biogeochemistry and microbial ecology. *Rapid Commun Mass Spectrom* 18(6):617–628.
10. White DC, Davis WM, Nickels JS, King JD, Bobbie RJ (1979) Determination of the sedimentary microbial biomass by extractible lipid phosphate. *Oecologia* 40(1):51–62.
11. Harvey HR, Fallon RD, Patton JS (1986) The effect of organic matter and oxygen on the degradation of bacterial membrane lipids in marine sediments. *Geochim Cosmochim Acta* 50(5):795–804.
12. Logemann J, et al. (2011) A laboratory experiment of intact polar lipid degradation in sandy sediments. *Biogeosciences* 8(9):2547–2560.
13. Schubotz F, Wakeham SG, Lipp JS, Fredricks HF, Hinrichs K-U (2009) Detection of microbial biomass by intact polar membrane lipid analysis in the water column and surface sediments of the Black Sea. *Environ Microbiol* 11(10):2720–2734.
14. Van Mooy BAS, et al. (2009) Phytoplankton in the ocean use non-phosphorus lipids in response to phosphorus scarcity. *Nature* 458(7234):69–72.
15. Lipp JS, Hinrichs K-U (2009) Structural diversity and fate of intact polar lipids in marine sediments. *Geochim Cosmochim Acta* 73(22):6816–6833.
16. Schouten S, Middelburg JJ, Hopmans EC, Sinninghe Damsté JS (2010) Fossilization and degradation of intact polar lipids in deep subsurface sediments: A theoretical approach. *Geochim Cosmochim Acta* 74(13):3806–3814.
17. Rossel PE (2009) Microbial communities performing anaerobic oxidation of methane: Diversity of lipid signatures and habitats. PhD thesis (Univ of Bremen, Bremen, Germany). Available at http://d-nb.info/994838808/34.
18. Middelburg JJ (1989) A simple rate model for organic matter decomposition in marine sediments. *Geochim Cosmochim Acta* 53(7):1577–1581.
19. D'Hondt S, Rutherford S, Spivack AJ (2002) Metabolic activity of subsurface life in deep-sea sediments. *Science* 295(5562):2067–2070.
20. Middelburg JJ, Vlug T, Van der Nat FJWA (1993) Organic matter mineralization in marine systems. *Global Planet Change* 8(1-2):47–58.
21. Rothman DH, Forney DC (2007) Physical model for the decay and preservation of marine organic carbon. *Science* 316(5829):1325–1328.
22. Heijnen JJ, Van Dijken JP (1992) In search of a thermodynamic description of biomass yields for the chemotrophic growth of microorganisms. *Biotechnol Bioeng* 39(8): 833–858.
23. Nauhaus K, Albrecht M, Elvert M, Boetius A, Widdel F (2007) In vitro cell growth of marine archaeal-bacterial consortia during anaerobic oxidation of methane with sulfate. *Environ Microbiol* 9(1):187–196.
24. Wegener G, Niemann H, Elvert M, Hinrichs K-U, Boetius A (2008) Assimilation of methane and inorganic carbon by microbial communities mediating the anaerobic oxidation of methane. *Environ Microbiol* 10(9):2287–2298.
25. Hoehler TM, Alperin MJ, Albert DB, Martens CS (1994) Field and laboratory studies of methane oxidation in an anoxic marine sediment: Evidence for a methanogen-sulfate reducer consortium. *Global Biogeochem Cycles* 8(4):451–463.
26. Simon M, Azam F (1989) Protein content and protein synthesis rates of planktonic marine bacteria. *Mar Ecol Prog Ser* 51:201–213.
27. Schippers A, Köweker G, Höft C, Teichert BMA (2010) Quantification of microbial communities in forearc sediment basins off Sumatra. *Geomicrobiol J* 27(2):170–182.
28. Schippers A, Kock D, Höft C, Köweker G, Siegert M (2012) Quantification of microbial communities in subsurface marine sediments of the Black Sea and off Namibia. *Front Microbiol* 3:16, 10.3389/fmicb.2012.00016.
29. Lin Y-S, Lipp JS, Elvert M, Holler T, Hinrichs K-U (2013) Assessing production of the ubiquitous archaeal diglycosyl tetraether lipids in marine subsurface sediment using intramolecular stable isotope probing. *Environ Microbiol*, 10.1111/j.1462-2920.2012.02888.x.
30. Dell'Anno A, Danovaro R (2005) Extracellular DNA plays a key role in deep-sea ecosystem functioning. *Science* 309(5744):2179.
31. Wegener G, et al. (2012) Assessing sub-seafloor microbial activity by combined stable isotope probing with deuterated water and ^{13}C-bicarbonate. *Environ Microbiol* 14(6): 1517–1527.
32. Corinaldesi C, Barucca M, Luna GM, Dell'Anno A (2011) Preservation, origin and genetic imprint of extracellular DNA in permanently anoxic deep-sea sediments. *Mol Ecol* 20(3):642–654.
33. Expedition 311 Scientists (2006) Site U1326. *Proceedings of the Integrated Ocean Drilling Program*, eds Riedel M, Collett TS, Malone MJ; Expedition 311 Scientists (Integrated Ocean Drilling Program Management International, Washington, DC), Vol 311, 10.2204/iodp.proc.311.104.2006.